Oxygen Reduction in Alkaline Media—a Discussion

Anna Ignaczak, Renat Nazmutdinov, Aleksej Goduljan, Leandro Moreira de Campos Pinto, Fernanda Juarez, Paola Quaino, et al.

Electrocatalysis

ISSN 1868-2529

Electrocatalysis
DOI 10.1007/s12678-017-0365-y

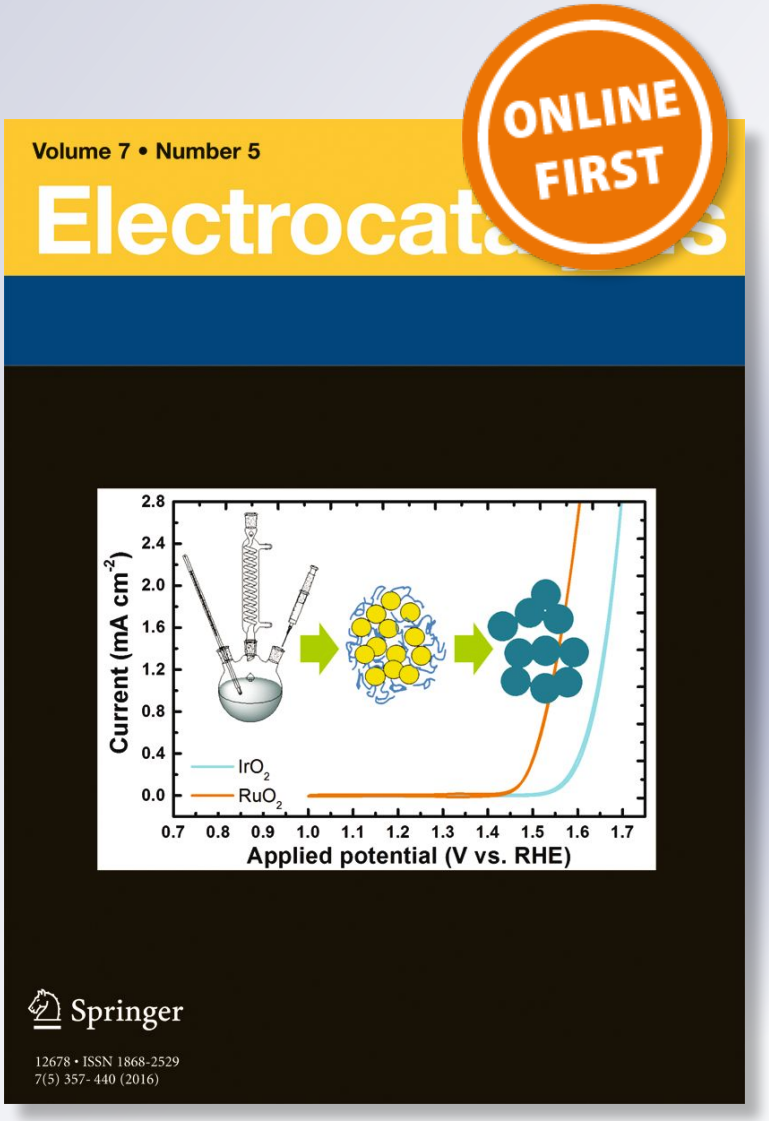

Springer

Electrocatalysis
DOI 10.1007/s12678-017-0365-y

ORIGINAL ARTICLE

Oxygen Reduction in Alkaline Media—a Discussion

Anna Ignaczak[4] · Renat Nazmutdinov[3] · Aleksej Goduljan[1] · Leandro Moreira de Campos Pinto[1,6] · Fernanda Juarez[1] · Paola Quaino[5] · Gustavo Belletti[5] · Elizabeth Santos[1,2] · Wolfgang Schmickler[1]

Abstract We propose a complete reaction sequence for oxygen reduction in alkaline solutions, in which the first two steps occur in the outer sphere mode. The oxygen-oxygen bond is broken in the third step, which involves adsorption of OH, which is desorbed in the last step. We have investigated the sequence by quantum-chemical methods and determined the energies of activation. Whether the reaction follows a four- or a two-electron mechanism, depends critically on the energy of adsorption of OH. We surmise that our mechanism holds on all electrodes which interact weakly with oxygen, in particular on gold, silver, and graphite. We explain, why Au(100) is a better catalyst than Au(111), why at high overpotentials the reaction on Au(100)reverts to a two-electron mechanism, and why this does not happen on silver.

Keywords Oxygen reduction · Alkaline fuel cells · DFT · Electron transfer

✉ Wolfgang Schmickler
wolfgang.schmickler@uni-ulm.de

[1] Institute of Theoretical Chemistry, Ulm University, 89069, Ulm, Germany

[2] Facultad de Matemática, Astronomía y Física, IFEG-CONICET Universidad Nacional de Córdoba, Córdoba, Argentina

[3] Kazan National Research Technological University, 420015, Kazan, Russian Federation

[4] Department of Theoretical and Structural Chemistry Faculty of Chemistry, University of Lodz, Pomorska 163/165, 90-236, Lodz, Poland

[5] PRELINE, Universidad Nacional del Litoral Santa Fe, Santa Fe, Argentina

[6] Instituto de Química Universidade Federal de Mato Grosso do Sul, Campo Grande, Brasil

Introduction

Like all good things, the special research unit *Elementary reaction steps in electrocatalysis: Theory meets Experiment* must come to an end. Within this endeavor we investigated *electron transfer in oxygen reduction* with the focus on alkaline media. In the following, we present our most important results and discuss them in the context of electrocatalysis. Since this communication marks the official end of our project, it takes the form of a review of our work with some new thoughts.

Oxygen reduction is of obvious importance, and there has been a huge amount of research, both experimental and theoretical, on this topic during the last decades, but most of this has been on acid solutions. The practical reason for this is the fact, that acid fuel cells are better developed because of the polymer membrane. As far as theory is concerned, the reason lies in a weakness of density functional theory (DFT), which nowadays is the prevalent theoretical method for studying electrochemical processes at the atomic level: DFT has great problems in treating ions and charge transfer. In acid solutions one can devise a reaction path, in which each step consists of a combined electron and proton transfer [1], so that both reactant and product are neutral. Thus, the thermodynamics—though not the kinetics—of these steps can be calculated by standard DFT.

Published online: 10 March 2017

Whether the reaction always proceeds by a series of combined electron-proton steps, is a different question, which is often ignored, but which has been well discussed in a recent article by Koper [2]. In alkaline solutions, protons, which can compensate the electronic charge, play no role. Therefore, the reaction proceeds through a series of steps with charged intermediates, which makes a treatment by pure DFT difficult.

The rest of this article is organized as follows: First, we discuss a few thermodynamic aspects, then we examine the relevance of inner and outer sphere electron transfer before we present a reaction path and look at each step from a theoretical point of view. Oxygen reduction is slow and limits the efficiency of many types of fuel cells. In acid media, platinum group metals are the best catalyst. In contrast, in alkaline solutions, metals like silver and gold are very effective. Therefore, our review focuses on these metals. In particular, we propose an explanation for an old puzzle: why Au(100) is a so much better catalyst than Au(111). The technical details of our calculations can be found in the Appendix.

A Few Thermodynamic Aspects

It is interesting to compare the thermodynamics of the first reaction steps in acid and in alkaline solutions. In the former case, the first step is usually:

$$O_2 + H^+ + e^- \rightarrow HO_2 \qquad (1)$$

If none of the reactants are adsorbed, i.e., if this reaction takes place in an outer-sphere mode, the standard equilibrium potential for this reaction is near 0 V RHE [3], which would imply a terrible overpotential of about 1.2 V. There are two ways to make the thermodynamics of this reaction better:

(1) Specific adsorption of the product HO_2; a free energy of adsorption ΔG_{ad} lowers the overpotential by $-\Delta G_{ad}/e_0$;
(2) A fast follow-up reaction which keeps the coverage with the adsorbate low [4] and shifts the equilibrium potential to higher values according to the Nernst equation. Obviously, the latter effect can shift the potential only by a few tenths of a volt, and is not sufficient to lower the overpotential to a reasonable value.

Therefore, in acid solutions, oxygen reduction requires a catalyst which binds the intermediate neither too weakly nor too strongly, and an adsorption energy of the order of -1 eV should be close to the optimal value. In fact, that is just the energy of adsorption of HO_2 on Pt(111) [5]. For Pd(111), another good catalyst, it is -1.15 eV, and for Au(111) and Ag(111), both bad catalysts in acid solutions, the values are –0.25 and –0.57 eV, respectively. A more complete analysis containing considerations for other metals as well is given in [6].

While acid solutions require a good, and usually expensive, catalysts, the situation on alkaline solutions is much more favorable. Here, the first step is:

$$O_2 + e^- \rightarrow O_2^- \qquad (2)$$

The overall reaction occurs with roughly the same speed on a variety of electrodes, among them gold and silver, which are cheap compared to platinum. It has therefore been suggested that this step takes place in the outer sphere mode [7]. This view is compatible with thermodynamic considerations: In the outer sphere mode, the standard equilibrium potential is about –0.3 V SHE, compared with a value of 0.4 V SHE for the overall reaction at pH 14. When this first step is slow and the subsequent steps are fast, the concentration of O_2^- is low, and for concentrations of the order of $10^{-6} - 10^{-7}$ M the overpotential is reduced to about 0.3 V, which is quite compatible with the onset potential observed on gold and silver [8–12]. The difference in reactivity between various metals would then not be caused by the first, but by the subsequent steps, which determine the concentration of O_2^- in front of the electrode.

Outer Sphere Versus Inner Sphere Mechanism

Oxygen reduction belongs to the class of electrocatalytic reactions, which proceed with different rates on different substrates. Therefore, there is no doubt that at least one of its steps must involve an adsorbate. However, this need not be the first and not even the rate-determining step. As we have discussed above, in alkaline solutions, the first step is often considered to be:

$$O_2 + e^- \rightarrow O_2^-$$

In principle, both the reactant and the product could be adsorbed, and this has been assumed in a variety of older publications see, e.g., [13]. But there are two arguments that speak against this: Firstly, it is very rare that a small adsorbate can exist in two different charge states on a given surface. Secondly, if the reaction takes place on a metal surface, its rate cannot be influenced by the electrode potential. Since the electric field does not penetrate into metals, the application of an external potential does not change the electronic energy of an adsorbate with respect to the Fermi level. There can be second-order effects like the interaction of the dipole moment of an adsorbate with the electric field in the double layer [14], but they are too weak to explain the strong dependence of the reaction rate on potential observed in practice. So at least one of the reactants must be in the outer sphere.

Usually, small adsorbates on metal surfaces are not charged; however, because of its strong electronegativity, oxygen is an exception. As we shall discuss below, on Ag(100) it is adsorbed in the form of the anion O_2^-, and both the inner sphere and the outer sphere mechanism can occur in paralell.

If a species is adsorbed from the solution depends on three factors: One is the energy of adsorption which the species has in the vacuum; this can be calculated by DFT. The other is the change in solvation energy as the particle is brought from the bulk of the solution to the adsorption site—this is the so-called potential of mean force (pmf). The third is the electrode potential, which has a particularly strong effect when an ion is adsorbed from the solution and discharged in the process.

We start by comparing the adsorption of O_2 on three metals which show rather different behavior, Au, Ag, Pt, choosing the (100) surface as an example. Figure 1 shows the change in the energy as the molecule approaches the surface; the energy in the vacuum has been set to zero. The molecule does not chemisorb on Au(100); there is a very shallow minimum of –7 meV at a distance of about 3 Å from the surface, but the electronic density of states (DOS) shows no effect of chemical binding at this point. At shorter distances, the energy increases, till finally the bond breaks with an activation energy of about 1.5 eV. This is the prototype of a chemically inert substrate, even though—as we shall discuss later—it is an excellent catalyst in alkaline solutions. On Ag(100), the molecule adsorbs with an energy of about –0.4 eV; an analysis of the DOS shows, that the adsorbed molecule has an excess charge of –0.7, which is corroborated by Bader analysis. We shall show later, that in the presence of an aqueous solution, the charge is lowered to -1 because of solvation effects. Pt(100) shows an even stronger adsorption energy of -0.9 eV, and a negative excess charge of about –0.47 both from Bader analysis and from the DOS. The stronger adsorption on Pt can be attributed to the interaction with the d band, which both on Ag and Au lies too low to play a role. The difference in the charge of the adsorbed oxygen on Pt and Ag is related to the work function, which is 5.69 eV for Pt(100) and 4.23 eV for Ag(100). Because of the higher work function Pt attracts electrons much stronger than Ag does, so there is less charge transfer from the metal to the adsorbate.

The interaction of water with metal surfaces is weak; therefore, we do not expect the pmf for oxygen to depend much on the nature of the electrode. We have calculated the pmfs explicitly for the O_2 molecule and the O_2^- ion on Ag(100). The results are shown in Fig. 2; they give the change in the energy of solvation as the particle approaches the electrode.

The pmf of both the molecule and the anion increase towards the surface, as their hydration becomes weaker. This effect is stronger for the molecule, where the pmf begins to rise at about 6 Å, than for the anion, where it even has a slight minimum near 5 Å before it starts to rise. Considering that the hydration energy of the anion is about –3.9 eV [3], the rise in energy towards the surface is moderate. In contrast, the rise of the pmf for the molecule is higher than the absolute value of the solvation energy in the bulk (about –0.16 eV). We attribute this to an exclusion effect: Water likes to form a hydrogen-bonded network on the surface, and expels the molecule, whose solvation shell is much weaker than that of the anion. We note that almost always, oxygen reduction takes place at potentials positive to the pzc, so that the anion experiences an additional force which attracts it towards the electrode.

Without going into detailed calculations, we may conclude that on Au(100) reaction Eq. 2 takes place in the outer sphere mode. On Pt(100), the adsorbed state is favorable, while on Ag(100), there is a competition between adsorption and solvation; we shall return to this question below.

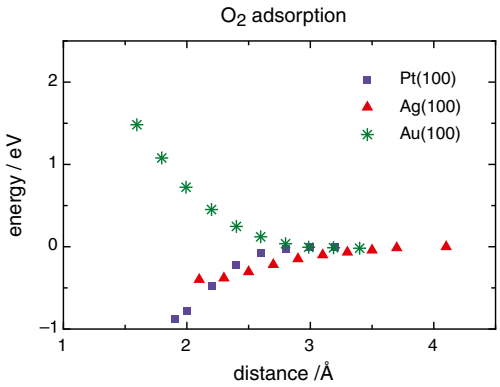

Fig. 1 Energy of a O_2 molecule near the (100) surfaces of Au, Ag, and Pt. For Pt and Ag, the *points* at the very left correspond to the adsorbed state

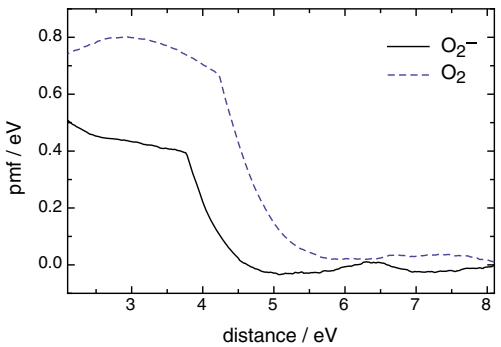

Fig. 2 Potentials of mean force for the approach of O_2^- and O_2 to an Ag(100) surface; after [16]

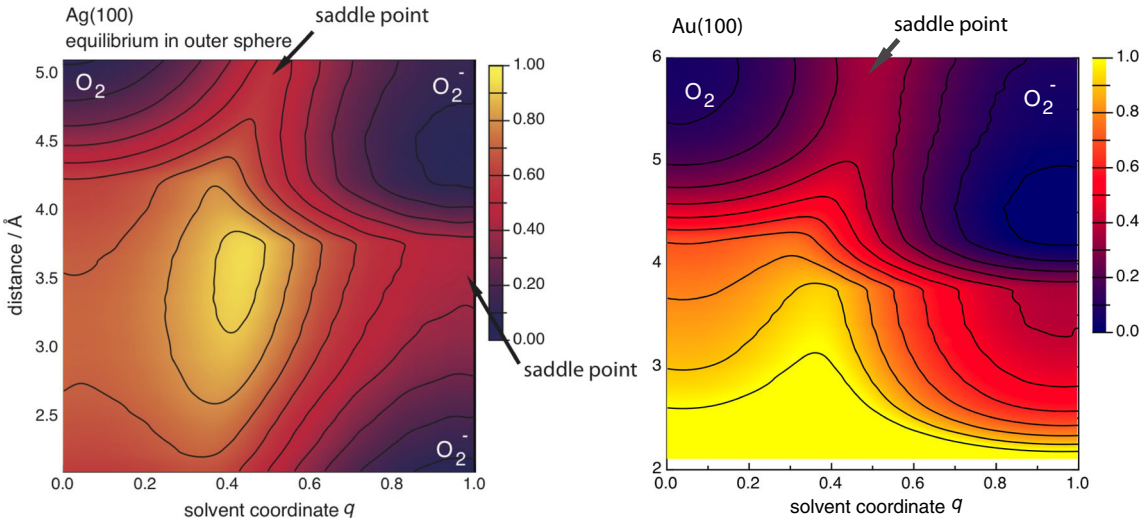

Fig. 3 Free energy surface for the reaction $O_2 + e^- \rightarrow O_2^-$ on Ag(100) and on Au(100). The electrode potential is for equilibrium in the outer sphere mode; after [15] and [16]

A Reaction Mechanism in Alkaline Solutions

In alkaline solutions, the overall reaction for the full reduction is:

$$O_2 + 2H_2O + 4e^- \rightarrow 4OH^- \tag{3}$$

On some surfaces, in particular on Au(111), the reaction stops after the transfer of two electrons, which results in:

$$O_2 + H_2O + 2e^- \rightarrow HO_2^- + OH^- \tag{4}$$

Numerous reaction mechanisms have been proposed; this is not the place to discuss them all, but we note that many of them must be discarded in the light of DFT calculations. This applies in particular to mechanisms that postulate two different forms of adsorbed oxygen molecules, or the adsorption of O_2 on gold as a first step. Details have been discussed in a previous communication [17], where we proposed the following mechanism:

$$O_2 + e^- \rightarrow O_2^- \tag{5}$$

$$O_2^- + H_2O + e^- \rightleftharpoons HO_2^- + OH^- \tag{6}$$

$$HO_2^- + H_2O \rightleftharpoons 2OH_{ad} + OH^- \tag{7}$$

$$OH_{ad} \rightarrow OH^- \tag{8}$$

The two electron mechanism stops after the second step; this is, for example, the case on Au(111). All of the steps in our reaction scheme have been suggested before; the novelty of our approach lies in the theoretical investigations of the various steps, which present a consistent picture.

Theoretical Investigation of the Reaction Steps

The First Electron Transfer

We have previously investigated the first step on Au(100) [15] and Ag(100) [16]. For the sake of completeness, we discuss these results here. During the last years, our group has developed a theory for the investigation of electrocatalytic reactions [18–21]. It is well documented in the literature, so it suffices to state that it involves a combination of DFT with our electron transfer theory. We often plot the results in the form of free energy surfaces for the reactant as a function of the distance of the reactant from the solvent, and of the solvent coordinate q. The latter is a concept derived from Marcus theory [22] and characterizes the state of the solvent. It takes on the value q, when the solvent would be in equilibrium with a reactant of charge $-q$ [23]. Outer sphere electron transfer takes place at a distance from the electrode, while q varies. For example, if the reaction $O_2 + e^- \rightarrow O_2^-$ takes place in the outer sphere mode, q changes from zero to unity.

From the considerations in the previous section, it is expected that on Au(100) the first step takes place in the outer sphere mode. As can be seen from the r.h.s. of Fig. 3, this is indeed the case. The surface shows two minima away from the surface: one centered at $q = 0$, which corresponds to the neutral molecule, and another one centered at $q = 1$ corresponding to the anion. More precisely, the minimum at $q = 0$ extends into a valley at larger distances; in contrast, the one at $q = 1$ is a proper minimum. On gold and silver, oxygen reduction takes place at potentials above the pzc, so the double-layer field attracts the ion towards the surface. The two minima are separated by an energy barrier of

about 0.5 eV, which coincides with the prediction of Marcus theory [24]: The free energy of solvation of the O_2^- anion in the bulk of the solution is –3.9 eV; about half of this is due to the slow solvent modes, the other half to the fast. Therefore, the energy of reorganization, which is caused by the slow modes, is about 2 eV; at zero overvoltage, Marcus theory predicts an activation energy of $\lambda/4$. Thus, with hindsight it we could have spared ourselves the DFT calculations and could have used Marcus theory right away.

On Ag(100), the situation is more complicated (see l.h.s. of Fig. 3). At equilibrium, there are three minima: two of them correspond to those observed on Au(100), and there is a third minimum for an adsorbed O_2^- centered at $q = 1$. Compared to the vacuum, the effect of solvation has increased the negative charge on the adsorbed oxygen to -1. The outer sphere electron transfer occurs in the same way as on gold, again with an activation energy of 0.5 eV. The O_2^- ion can be adsorbed on the Ag(100) surface, where it has about the same energy—note that these calculations are also for the case where the reaction in the outer sphere is in equilibrium. The energy of activation for the adsorption is about 0.4 eV. Note that there is no favorable reaction path that leads from the molecule O_2 directly to the adsorbed O_2^-; to become adsorbed, the first electron transfer must take place in the outer sphere. The reason for this can be seen in the pmf for the molecule (see Fig. 2), which rises by about 0.8 eV near the surface and prevents the approach of the molecule.

The application of an overpotential η affects only the anion in the outer sphere, whose energy is lowered by $-e_0\eta$; the energy of the anion on the surface is practically unchanged, and it becomes unstable with respect to the outer sphere position—see Fig. 4. So we conclude that

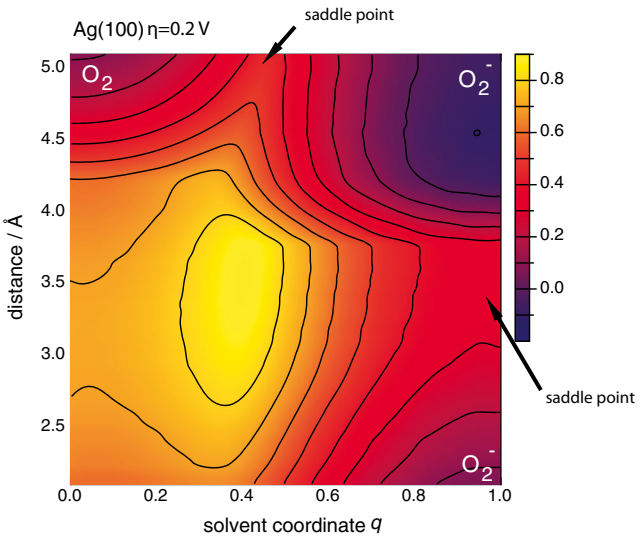

Fig. 4 Free energy surface for the reaction $O_2 + e^- \rightarrow O_2^-$ on Ag(100) on application of an overpotential of 0.2 V. After [16]

on Ag(100) the first electron transfer also takes place in the outer sphere mode, but near the equilibrium potential there will be O_2^- adsorbed on the surface, which may exchange with the outer sphere position, and which becomes unstable on the application of an overpotential. Overall, the adsorbed species should have little effect on the rate. This explains why oxygen reduction on Au(100) and Ag(100) occur in a similar way.

It would be natural to perform the same calculations for Pt(100); however, they would be irrelevant. On platinum oxygen reduction is determined by the adsorption/desorption of OH, which takes place in the same potential region. This is evidenced by the fact that it is independent of pH, when the current is plotted on the RHE scale [25]—see also the previous works [26, 27]. Therefore, experimental data reveal nothing about the oxygen reduction as such. OH adsorption is favored over oxygen by two aspects: (1) The adsorption energy of OH from the vacuum is about –2.3 V [21, 28, 29] and thus lower than that of O_2, and the pmf for the adsorption of OH^- rises only by 0.3 V at the surface [21]. Experimentally it has been found to be very fast [30], and this is supported by theory [21]. The adsorption of OH effectively blocks the surface of platinum for oxygen reduction. In addition, at high potential oxide formation also plays an unfavorable role. Thus, oxygen reduction on platinum takes place by a different mechanism and cannot be compared with silver and gold.

The Second Electron Transfer

So on Au and Ag the first electron transfer takes place in the outer sphere mode. At the beginning of the subsequent step:

$$O_2^- + H_2O + e^- \rightleftharpoons HO_2^- + OH^-$$

the O_2^- ion is in the outer sphere and surrounded by water. Practically always the electrode surface will be positively charged, so that the generated anions are attracted to the double-layer region. Since the products do not exist in an adsorbed form, we have assumed that this reaction takes place in the outer sphere mode. Formally, the reaction can be considered as an outer sphere electron transfer coupled with a bond rearrangement. The corresponding theory has been developed by Koper and Voth [31], by Schmickler [32], and by Santos, Koper, Schmickler [33] and has been applied to specific examples by Ignaczak and Schmickler [34].

The reaction can be considered as an H-atom transfer from the water molecule to the O_2^- with a simultaneous electron transfer to the OH radical. Therefore, the distance between O_2^- and the nearest H-atom of water was taken as the reaction coordinate. Following the guidelines of theory, we have calculated free energy curves for the initial and the final states as a function of this coordinate.

Table 1 Energy of activation E_a in eV for reaction Eq. 6 for various numbers of explicit water molecules

Reactant	$O_2(H_2O)_2^{2-}$	$O_2(H_2O)_4^{2-}$	$O_2(H_2O)_6^{2-}$
E_a	0.027	0.19	0.06

Because of the charges on the reactants and products, DFT in the slab geometry is unsuitable. Therefore we have investigated this reaction with the Gaussian suite of programs, which allows calculations with ions. Solvation is important for electron transfer; so we have investigated this reaction with a variable number (1, 2, 4, and 6) of explicit water molecules; the rest of the solvation shell was treated by the polarizable continuum model. The electrode serves only as an electron donor, therefore, it was not explicitly considered. In the calculations, the O–H distance was scanned, while the other coordinates were allowed to relax. Thus, the motion of the H-atom was treated as purely classical. As starting geometry, we took the optimized initial cluster $O_2(H_2O)_n^-$. The final state includes partially hydrated HO_2^- and OH^- ions coupled through H-bonds. This intermediate is assumed to dissociate with the formation of spatially separated HO_2^-(solv) and OH^-(solv).

The results depend on the number of water molecules that treated explicitly—see Table 1. Here, we show the free energy curve for equilibrium conditions calculated with six explicit water molecules—see Fig. 5. Independent of the number of water molecules treated explicitly, the barrier is very low, so that the reaction should proceed fast in both directions, and should always be in equilibrium.

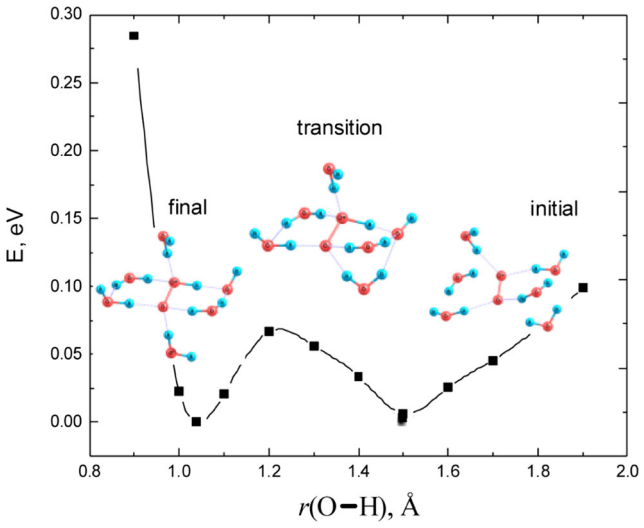

Fig. 5 Free energy curve for the reaction $O_2^- + H_2O + e^- \rightleftharpoons HO_2^- + OH^-$ calculated with 6 explicit water molecules; the barrier height is 0.06 eV; taken from [17]

Breaking of the Oxygen-Oxygen Bond

The first two reactions in our scheme take place in the outer sphere; hence, they do not depend on the electrode material as long as this is a good conductor and is not covered by an inhibiting species. So far, two electrons have been passed, and up to now, the mechanism is the same for a good four-electron catalyst as for a bad two-electron catalyst. The next step:

$$HO_2^- + H_2O \rightleftharpoons 2OH_{ad} + OH^-$$

involves two adsorbed OH. Hence, it depends on the electrode material, and it is here that the paths for Au(111) and Au(100) diverge: On the former, the reaction stops before this step takes place, on the latter, it continues. This reaction once again shows the importance of OH adsorption in alkaline solutions. For the above reaction to be effective, OH adsorption must be neither so strong, that it blocks the electrode, nor so weak that it becomes energetically unfavorable.

We have modeled this reaction explicitly on Au(100); later we shall compare OH adsorption on Au(100) and Au(111) to explore the difference. This step involves the breaking of the oxygen–oxygen bond, a negative excess charge, and the simultaneous adsorption of two OH radicals, while one OH^- stays in the solution. Because of the negative excess charge we chose the Gaussian suite of programs for the calculations, and modeled the Au(100) surface by a gold cluster of 24 atoms (see Fig. 6). Since the cluster is finite, the surface sites are not all equivalent. Solvation was treated by the PCM model. If we leave all of the atoms free to move, they drift to the side of the cluster; this is unwanted since the center of the cluster is the best representation of the (100) surface. Therefore, in all calculations, the OOH^- ion was kept at a bridge site with the O–O bond perpendicular to the metal surface. For the oxygen atom of the water molecule, we tried several possible initial structures, and so far, a position at the neighboring bridge site gave the best results, i.e., the lowest energy—see Fig. 6. Note that in the initial structure, one O-H bond in the H_2O molecule is stretched toward the OOH^- ion.

As reaction coordinate, we chose the distance between the two oxygen atoms in the HO_2^- anion. We first performed the calculations without the gold surface. In this case, the reaction is endothermic with $\Delta H \approx 2.4$ eV and $\Delta G \approx 2.1$ eV; this is in reasonable agreement with an estimate of $\Delta H \approx 2.2$ eV obtained from tables [3]. Obviously, the spontaneous breaking of the O–O bond in solution will not occur. In contrast, on the Au(100) surface the reaction is exothermic by about 0.3 eV, and the barrier is 0.68 eV (see Fig. 7). Note that the calculations correctly result in two adsorbed OH radicals and an OH^- ion in solution. The energies contain the purely electronic energies resulting from

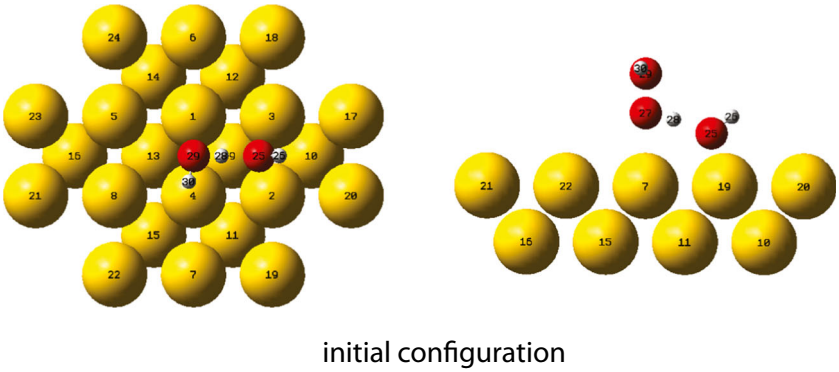

Fig. 6 Initial configuration for the reaction $HO_2^- + H_2O \rightleftharpoons 2OH_{ad} + OH^-$; after [17]

DFT and the solvation energies, which have the nature of a free energy.

Because of the simplicity of the model system and the approximations involved, these calculations are not quantitative. In particular, the activation energy obtained here cannot be compared directly with the somewhat lower value of the first step, which has been calculated by a different method. However, our results clearly demonstrate that the breaking of O–O bond, which determines if the overall reactions involves four or only two electrons, requires a strong adsorption of OH on the electrode surface. We believe that this is the key to understanding the role of the catalysts.

A recent paper by Calle-Vallejo et al. [35] also points out the importance of OH adsorption for bond breaking; however, their arguments are mainly based on the adsorption of OOH on various gold surfaces and, thus, differ from ours in some details.

Desorption of OH

After the first two steps, the reaction is dominated by the adsorption and desorption of OH. On the one hand, the adsorption of OH must be sufficiently strong to make reaction Eq. 7 exergonic, but it must be so weak that finally the adsorbed OH can be released as OH^- to the solution. For this purpose it is helpful if the adsorption of OH depends on the coverage with OH; this ensures that over a broad range of coverage there are sites on which OH can be adsorbed with a medium strength.

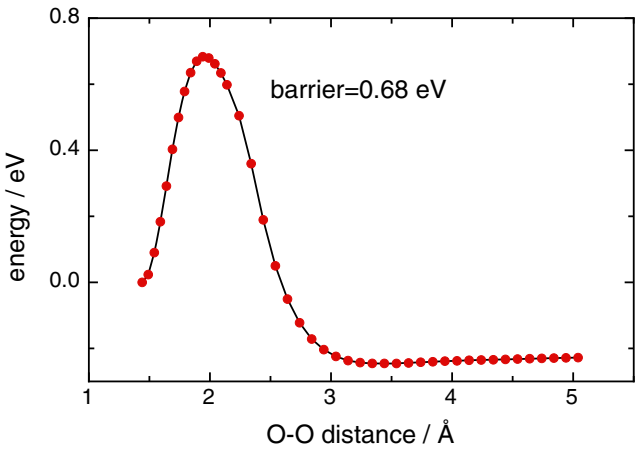

Fig. 7 Energy curve for the bond breaking step on a Au(100) surface; after [17]

One of the purposes of our investigation was to seek an explanation, why on Au(111) the reaction stops after the second step, while on Au(100) all calculated the energy of adsorption of OH on both gold surfaces for various coverages. The results are shown on the left hand side of Fig. 8. The energies depend on the coverage, but adsorption on Au(100) is more favorable than on Au(111) by between 0.2 and 0.4 eV. Calculating adsorption energies of OH from aqueous solutions is somewhat problematic, since the adsorbate can form hydrogen bonds with the adjacent layer of water. Therefore, we have performed additional calculation for adsorption in the presence of a layer of water, and have included van der Waals corrections—see right hand side of Fig. 8. Adsorption on Au(100) remained more favorable by about the same amount of energy as before. The absolute values of the two calculations cannot be compared, since the latter includes a layer of water in its reference state. In the presence of water the energy rises with coverage; here, the adsorbed OH forms hydrogen bonds with water and cannot profit from interaction with nearest neighbors. Without water, for Au(111), the energy at first drops with coverage before rising, while on Au(100) it remains constant before rising. For the electrochemical situation, the calculations with water are more realistic, so we conclude that the energy rises with coverage. As mentioned above, this is advantageous, since it ensures that there will be empty sites with a suitable energy over a broad range of potentials.

OH adsorption on gold has been investigated by a fair number of researchers, principally on Au(111) [5, 28, 36], and most obtained a slightly higher, near –1.8 eV, value than we did. This difference can be traced to a different choice of pseudopotentials. However, the important point is that those

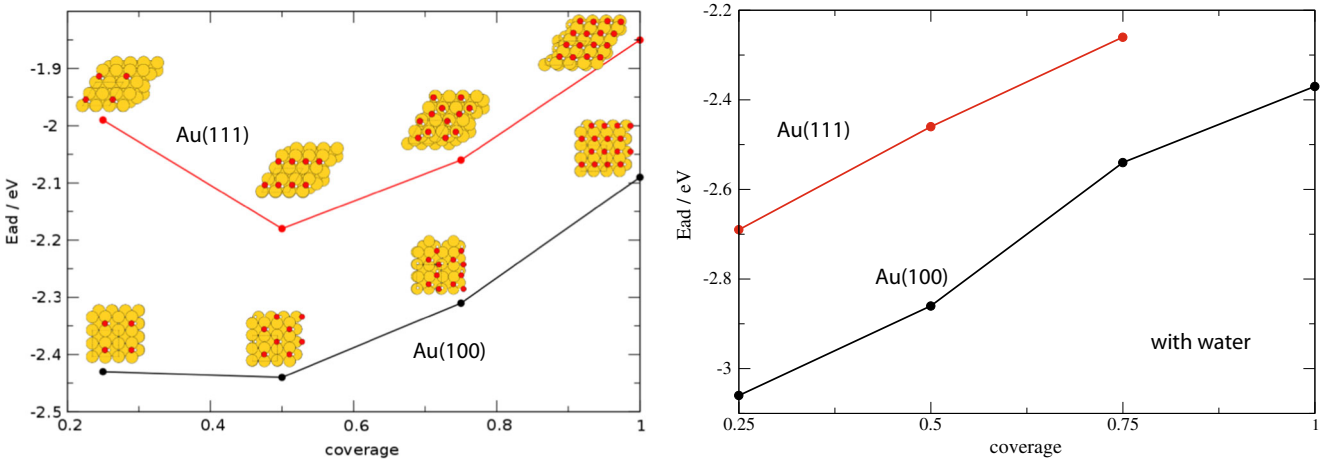

Fig. 8 Energy of adsorption of OH from the vacuum for Au(100) and Au(111) for various coverages; *left* without water, *right*:with a monolayer of water. The absolute values for the two sets of calculations cannot be compared since they have different reference states

researchers who investigated both surfaces also obtained a difference of about 0.4 eV at low coverages, with Au(100) being the more favorable surface [37, 38].

Experimentally, it is well established that OH adsorption is stronger on Au(100) than on Au(111) [39, 40], although the cyclic voltammograms obtained in various groups differ in details. The adsorption of OH on Au(111) has been studied quantitatively by Chen and Lipkowski [41]; Fig. 3 of their work clearly shows that the coverage is low in the region relevant for oxygen reduction. Unfortunately, a similar quantitative study for Au(100) is missing, so we have to rely on the evidence from cyclic voltammograms.

At large overpotentials oxygen reduction on Au(100) reverts to the two-electron mechanism—see for example [11] and references therein. This means that reaction (7) no longer occurs in this region. At a first glance, this reaction seems to be independent of the electrode potential, since it involves no charged species. However, this is only true if the adsorbed OH is fully discharged, or, equivalently, that the electrosorption valency for the reaction $OH^- \rightarrow OH_{ad} + e^-$ is -1. Measuring electrosorption valencies requires very precise measurements. For Au(111) such experiments have been reported in the already cited article by Chen and Likpkowski [41]; especially for low electrode potentials they obtained values substantially higher than -1, which indicates that the adsorbed OH carries a sizable negative charge. This is in line with our DFT result, where at low coverages adsorbed OH both on Au(100) and Au(111) has a Bader charge of about –0.4. Therefore, with decreasing potential, the energy of the adsorbed OH become higher, and the free energy of reaction (7) rises accordingly and becomes less favorable. At the same time, the positive charge, which attracts the HO_2^- ion towards the surface, becomes smaller and inverts at the pzc, so that this anion can escape towards the bulk. We surmise that it is a combination of these two effects which blocks reaction (7). Finally, we note that on silver, the pzc is much more negative than on gold; for this reason, we believe, the four-electron mechanism persists even at high overpotentials [8]

Conclusions

In this work, we have presented a consistent mechanism for oxygen reduction in alkaline media based on quantum-chemical calculations. In our model, the first two steps follow an outer sphere electron transfer, and we have analyzed these in detail for Au(100) and Ag(100). These steps should be independent of the electrode material, as long as the surface is not blocked by adsorbates. In particular, the routes for the two- and four-electron mechanism are the same up to this point. The oxygen-oxygen bond is broken in the third step, which involves the adsorption of OH. This critical step requires an adsorption strength of the right order of magnitude: It should be sufficiently strong to break the bond, but not so strong as to block the surface. It is favorable if the adsorption becomes weaker with increasing coverage, so that part of the surface is free.

Our results explain the following features:

(1) Why on Au(100) the reaction the reaction goes all the way, while on Au(111) it stops after the transfer of two electrons.
(2) Why on Au(100) at high overpotentials the reaction also stops after the second step, and
(3) why this does not happen on silver. Of course, these explanations are still somewhat tentative, but they follow naturally from our model and are consistent with experimental data.

This mechanism should hold whenever oxygen does not adsorb on the electrode. Graphite is another nice example besides gold: Yang and McCreery [42] showed that on clean graphite the reduction $O_2 + e^- \rightarrow O_2^-$ is reversible, and the reverse can be observed in the backward sweep of a cyclic voltamogram. On this surface, oxygen does not adsorb, and the reaction stops after the transfer of two electrons. Since the second step is very fast, the first two steps can be reversed, so that the oxidation of O_2^- can be observed when the direction of the potential scan is reversed.

As the example of Ag(100) shows, our mechanism can also hold when the adsorption of oxygen is moderately strong. So what happens if it is really strong? It is difficult to think of a mechanism in which the strong adsorption of O_2, be it neutral or negatively charged, is favorable. However, in practice metals which adsorb oxygen strongly tend to adsorb OH even more strongly, so that oxygen reduction is then governed by the kinetics of OH adsorption/desorption, as seems to be the case on platinum.

Finally, we note, that in several non-aqueous solvents, the generation of O_2^- is the first step in oxygen reduction. Therefore, it is natural to extend our work to such solvents.

Acknowledgments Financial support by the Deutsche Forschungsgemeinschaft (FOR 1376) is gratefully acknowledged. E.S. and W.S. thank CONICET for continued support. E. S. acknowledges PIP-CONICET 112-2010001-00411, and PICT- 2012-2324 (Agencia Nacional de Promoción Cientiífica y Tecnolóogica, FONCYT, prééstamo BID) for support. L.M.C.P. thanks the Conselho Nacional de Desenvolvimento Científico e Tecnológico (CNPq/CsF 203178/2014-9) for a fellowship. A generous grant of computing time from the Baden-Württemberg grid is gratefully acknowledged. P.Q. and G.B. thank PICT-2014-1084, CONICET and UNL for support.

Appendix: Theoretical background

Technical Details of the DFT Calculations

Oxygen on Silver, Platinum, and Gold Periodic density functional theory (DFT) calculations were performed using the DACAPO [43] code with implemented Vanderbilt [44] ultrasoft pseudopotentials for the representation of the atomic cores. A PBE (Perdew, Burke, Ernzerhof) [45] functional and a set of plane waves with a cutoff energy of 350 eV (400 eV for the density) were chosen to describe the valence electrons. Brillouin zone integration [46] was performed using 4 k-points in the x- and y-directions respectively and 1 k-point in the z-direction. The surface was represented by 3 layers of metal atoms, and a 3×3 unit cell was employed.

OH on Gold All calculations were performed using the VASP code [47, 48]. The correlation and exchange functionals were described within the generalized gradient approximation (GGA) in the Perdew, Burke and Ernzerhof (PBE) flavor [45]. The electron-ion interactions were represented through ultrasoft pseudopotentials [44], and a plane wave basis set was used to describe the valence electrons. The basis set was expanded to a kinetic energy cutoff of 500 eV. Brillouin zone integration was performed using (10x10x1) k-point MonkhorstPack [49] grid . We used a dipole-correction scheme [50] to avoid slab-slab interactions. To investigate the adsorption of OH as a function of the coverage, both surfaces Au(100) and Au(111) were modelled by a (2 x 2) supercell with four metal layers. In all the calculations 15 A of vacuum were considered. For the relaxations, the two bottom layers were fixed at the calculated nearest-neighbour distance corresponding to bulk, and all the other layers plus the OH were allowed to relax. To mimic the aqueous media, a water layer was considered on the previous systems at each coverage. In order to take into account van der Waals interactions, the DFT-D3 [51] approach of Grimme [52] was used, which consists of adding a semiempirical dispersion potential to the conventional Kohn–Sham DFT energy.

Reaction 6 The DFT calculations were performed using the b3lyp functional as implemented in the Gaussian 09 program suite [53]; the standard 6-311++g(d, p) basis set was employed to describe the O and H atoms. The spin-polarized formalism was used to treat open shell molecules. Local hydration was considered explicitly by including of several water molecules into the nearest solvation sheath of the ions, while long-range solvent effects were addressed by the Polarized Continuum Model (PCM) taking a value of 78 as static dielectric constant. The molecular geometry in initial and final states was fully optimized without any restrictions.

Breaking of the Oxygen-Oxygen Bond These calculations were performed using the Gaussian 09 suite [53]. The Au(100) surface was modeled a the metal cluster composed of two layers of gold atoms (16+8) arranged according to the fcc structure typical for gold with the nearest-neighbor distances Au-Au fixed at the experimental value of 2.88 Å, and was kept unchanged in all calculations. The H_2O OOH^- system was first optimized in the bulk solution and then placed above the Au_{24} cluster, as shown in Fig. 6. The potential energy surface presented in Fig. 7 was then obtained by systematically stretching the O–O bond of the OOH^- ion and optimizing other parameters of the system undergoing adsorption. In the potential energy scan, some constraints were applied: the metal cluster was kept rigid and the O–O bond of the OOH^- anion was kept always perpendicular to the surface at the central bridge site of the Au24 cluster. In all calculations, the PBE1PBE hybrid functional [45] was used together with the 6-31++G(d,p)

basis set for the H_2O OOH^- system, the pseudopotential LANL1DZ for the metal cluster, and the polarizable continuum model (PCM) for the solvent (water).

Technical Details of the Molecular Dynamics

To calculate the PMF canonical ensemble (constant NVT) steered-molecular dynamics simulation was conducted for 1 ns at 298 K on a simulation box containing a Ag(100) slab with three metal layers (thickness 4.09 Å), an ensemble of 470 water molecules, and the O_2 or O_2^- species. Previously, an equilibration run of 700 ps was carried out. Periodic boundary conditions were set in the x and y directions, and the Ewald summation method was used to handle with long-range electrostatic interactions.

Well-known 12-6 Lennard-Jones pairwise potential was used to model the interactions between the species. For the water, we used the SPC/E (extended simple point charge) model and the corresponding parameters for the oxygen and hydrogen were taken from Yoshida et al. [54]. The Lennard-Jones parameters for silver were taken from Agrawal et al. [55] and for the O_2 and the O_2^- species the parameters were taken from Poling et al. [56] and Shen et al. [57], respectively. The cross interactions were computed through the Lorentz-Berthelot mixing rules, $\epsilon_{ij} = \sqrt{\epsilon_{ii}\epsilon_{jj}}$, and $\sigma_{ij} = (\sigma_{ii} + \sigma_{jj})/2$.

All simulations were performed using the LAMMPS (large-scale atomic/molecular massively parallel simulator) code [58] with a time step equal to 2.0 fs. The average temperature of 298 K was maintained by using a Nose-Hoover thermostat with a relaxation time of 0.1 ps.

References

1. K. Nørskov, J. Rossmeisl, A. Logadottir, L. Lindquist, J.R. Kitchin, T. Bligaard, H. Jonsson, J. Phys. Chem. B **108**, 1 (2004)
2. M.T.M. Koper, Chem. Sci. **4**, 2710 (2013)
3. A. Bard, R. Parsons, J. Jordan (eds.), *Standard Potentials in Aqueous Solutions* (Marcel Dekker, New York, 1985)
4. W. Schmickler, Chem. Phys. Chem. **14**, 881 (2013)
5. T.H. Yu, T. Hofmann, Y. Sha, B. Merinov, D. Myers, C. Heske, I. Godard W. A., Phys. Chem. C **117**, 26598 (2013)
6. P. Quaino, F. Juarez, E. Santos, W. Schmickler, Beilstein J. of Nanotechnology **5**, 846 (2014)
7. N. Ramaswamy, S. Mukerjee, doi:10.1155/2012/491604, and references therein (2012)
8. B.B. Blizanac, P.N. Ross, N.M. Markovic, J. Phys. Chem. **110**, 4735 (2006)
9. N.M. Marcovic, R.R. Adzic, V.B. Vesovic, J. Electroanal. Chem. **163**, 121 (1984)
10. N.M. Marcovic, R.R. Adzic, V.B. Vesovic, J. Electroanal. Chem. **165**, 105 (1983)
11. S. Strbac, R.E. Adzic, Electrochim. Acta **41**, 2903 (1996)
12. D. Mei, Z. Da He, Y. Li Zheng, D. Chuan Jiang, Y.-X. Chen, Phys. Chem. Chem. Phys. **16**, 13762 (2014)
13. T.J. Schmidt, V. Stamenkovic, M. Arenz, N.M. Markovic, Jr. Ross P. N., Electrochim. Acta **47**, 3765–3776 (2002)
14. M. Giesen, G. Beltramo, S. Dieluweit, J. Müller, H. Ibach, W. Schmickler, Surf. Sci. **595**, 127 (2005)
15. P. Quaino, N.B. Luque, R. Nazmutdinov, E. Santos, W. Schmickler, Angew. Chem. Int. Ed. **52**, 12459 (2012)
16. A. Goduljan, L. Moreira de Campos Pinto, F. Juarez, E. Santos, W. Schmickler, ChemPhysChem **17**, 500 (2016)
17. A. Ignaczak, R. Nazmutdinov, A. Goduljan, L. Moreira de Campos Pinto, F. Juarez, P. Quaino, E. Santos, W. Schmickler, Nano Energy **26**, 558564 (2016)
18. E. Santos, A. Lundin, K. Pötting, P. Quaino, W. Schmickler, Phys. Rev. B. **79**, 235436 (2009)
19. E. Santos, P. Quaino, W. Schmickler, PCCP **14**, 11224 (2012)
20. E. Santos, W. Schmickler, in *Fuel Cell Catalysis: a Surface Science, Approach*, ed. by M. Koper, *Electrochemical Electron Transfer: from Marcus Theory to Electrocatalysis* (Wiley, Hoboken, 2009)
21. L.M.C. Pinto, P. Quaino, M.D. Arce, E. Santos, W. Schmickler, Chem. Phys. Chem. **15**, 2002 (2014)
22. R.A. Marcus, J. Chem. Phys. **24**, 966 (1956)
23. W. Schmickler, E. Santos, *Interfacial Electrochemistry*, 2nd edn. (Springer Verlag, Berlin, 2010)
24. R.A. Marcus, J. Phys. Chem. **67**, 853,2889 (1963)
25. M.F. Li, L.W. Liao, D.F. Yuan, D. Mei, Y.-X. Chen, Electrochim. Acta **110**, 780789 (2013)
26. J.X. Wang, N.M. Markovic, R.R. Adzic, J. Phys. Chem. B **108**(108), 4127–4133 (2004)
27. N.M. Markovic, H.A. Gasteiger, Jr. Ross P. N., J. Phys. Chem. **100**, 6715–6721 (1996)
28. D.C. Ford, Y. Xu, M. Mavrikakis, Surf. Sci **587**, 159 (2005)
29. A. Michaelides, P. Hu, J. Chem. Phys. **114**, 513 (2001)
30. M.J.T.C. van der Niet, N. Garcia-Araeza, J. Hernández, J.M. Feliu, M.T.M. Koper, Catalysis Today **202**, 105113 (2013). and several references therein
31. M.T.M. Koper, G.A. Voth, Chem. Phys. Lett. **282**, 100 (1998)
32. W. Schmickler, Chem. Phys. Lett. **317**, 458 (2000)
33. E. Santos, M.T.M. Koper, W. Schmickler, Chem. Phys. Lett. **419**, 421 (2006)
34. A. Ignaczak, W. Schmickler, J. Electroanal. Chem. **554–555**, 201 (2003)
35. H. Li, Y. Li, M.T.M. Koper, F. Calle-Vallejo, J. Am. Chem. Soc. **136**, 15694–15701 (2014)
36. S. Kandoi, A.A. Gokhale, L.C. Grabow, J.A. Dumesic, M. Mavrikakis, Catalysis Lett **93**, 93 (2004)
37. P. Vassilev, M. Koper, J. Phys. Chem. C **111**, 2607 (2007)
38. A.M. Pessoa, J.L.C. Fajín, J.R.B. Gomes, M.N.D.S. Cordeiro, Surf. Sci. **606**, 69 (2012)
39. A. Prieto, J. Hernandez, E. Herrero, J. Feliu, J. Solid State Electrochem. **7**, 599 (2003)
40. R.R. Adzic, N.M. Marcovic, V.B. Vesovic, J. Electroanal. Chem. **165**, 105 (1984)
41. A. Chen, J. Lipkowski, J. Phys. Chem. B **103**, 682 (1999)
42. H.-H. Yang, R.L. McCreery, J. Electrochem. Soc. **147**, 3420 (2000)
43. S.R. Bahn, K.W. Jacobsen, Comput. Sci. Eng. **4**, 56 (2002)
44. D. Vanderbilt, Phys. Rev. B **41**, 7892 (1990)
45. J.P. Perdew, K. Burke, M. Ernzerhof, Phys. Rev. Lett. **77**, 3865 (1996)
46. D.J. Chadi, M.L. Cohen, Phys. Rev. B **8**, 5747 (1973)
47. G. Kresse, J. Hafner, Phys. Rev. B **47**, 558 (1993)
48. G. Kresse, J. Hafner, Phys. Rev. B **49**, 14251 (1994)
49. H.J. Monkhorst, J.D. Pack, Phys. Rev. B **13**, 5188 (1976)
50. L. Bengtsson, Phys. Rev. B. **59**, 12301 (1999)

51. S. Grimme, J. Antony, S. Ehrlich, H.A. Krieg, J. Chem. Phys. **132**, 154104 (2010)
52. S. Grimme, J. Comput.Chem. **27**, 1787–1799 (2006)
53. M.J. Frisch, G.W. Trucks, H.B. Schlegel, G.E. Scuseria, M.A. Robb, J.R. Cheeseman, G. Scalmani, V. Barone, B. Mennucci, G.A. Petersson, H. Nakatsuji, M. Caricato, X. Li, H.P. Hratchian, A.F. Izmaylov, J. Bloino, G. Zheng, J.L. Sonnenberg, M. Hada, M. Ehara, K. Toyota, R. Fukuda, J. Hasegawa, M. Ishida, T. Nakajima, Y. Honda, O. Kitao, H. Nakai, T. Vreven, Jr. Montgomery J. A., J.E. Peralta, F. Ogliaro, M. Bearpark, J.J. Heyd, E. Brothers, K.N. Kudin, V.N. Staroverov, T. Keith, R. Kobayashi, J. Normand, K. Raghavachari, A. Rendell, J.C. Burant, S.S. Iyengar, J. Tomasi, M. Cossi, N. Rega, J.M. Millam, M. Klene, J.E. Knox, J.B. Cross, V. Bakken, C. Adamo, J. Jaramillo, R. Gomperts, R.E. Stratmann, O. Yazyev, A.J. Austin, R. Cammi, C. Pomelli, J.W. Ochterski, R.L. Martin, K. Morokuma, V.G. Zakrzewski, G.A. Voth, P. Salvador, J.J. Dannenberg, S. Dapprich, A.D. Daniels, O. Farkas, J.B. Foresman, J.V. Ortiz, J. Cioslowski, D.J. Fox, *Gaussian 09, Revision B.01* (Gaussian, Inc., Wallingford CT, 2010)
54. K. Yoshida, T. Yamaguchi, A. Kovalenko, F. Hirata, J. Phys. Chem. B **106**, 5042 (2002)
55. P.M. Agrawal, B.M. Rice, D.L. Thompson, Surf Sci. **515**, 21 (2002)
56. B.E. Poling, J.M. Prausnitz, J.P. O'Connell, *Properties of Gases and Liquids*, 5th edn. (McGraw-Hill Education, New York, 2001)
57. J. Shen, C.F. Wong, J.A. McCammon, J. Comput. Chem. **11**, 1003 (1990)
58. S. Plimpton, Fast parallel algorithms for short–range molecular dynamics. J. Comput. Phys. **117**, 1 (1995). http://lammps.sandia.gov